

Supplementary Information

Sample	Initial discharge capacity [Ah kg ⁻¹]	Discharge capacity after <i>n</i> cycles [Ah kg ⁻¹]				Loss after 200 cycles [%]
		50	100	200	250	
LiAl _{0.02} Fe _{0.98} PO ₄	165	163	162	159	158	4
LiAl _{0.05} Fe _{0.95} PO ₄	154	151	149	146	142	5
LiAl _{0.07} Fe _{0.93} PO ₄	138	132	130	125	125	9
LiMn _{0.02} Fe _{0.98} PO ₄	162	160	159	158	157	2
LiMn _{0.05} Fe _{0.95} PO ₄	164	162	161	161	160	2
LiMn _{0.07} Fe _{0.93} PO ₄	156	155	154	152	151	3
LiNi _{0.02} Fe _{0.98} PO ₄	151	149	148	144	141	5
LiNi _{0.05} Fe _{0.95} PO ₄	137	134	132	118	113	14
LiNi _{0.07} Fe _{0.93} PO ₄	168	167	166	165	165	2
LiTi _{0.02} Fe _{0.98} PO ₄	164	163	163	153	153	7
LiTi _{0.05} Fe _{0.95} PO ₄	141	140	138	0	0	100
LiTi _{0.07} Fe _{0.93} PO ₄	159	156	153	148	147	7
LiZn _{0.02} Fe _{0.98} PO ₄	168	166	165	159	0	5
LiZn _{0.05} Fe _{0.95} PO ₄	138	135	133	112	0	19
LiZn _{0.07} Fe _{0.93} PO ₄	159	154	151	141	0	11

Table S1. Summary of the cycling performance tests of the different samples.

– 2 –

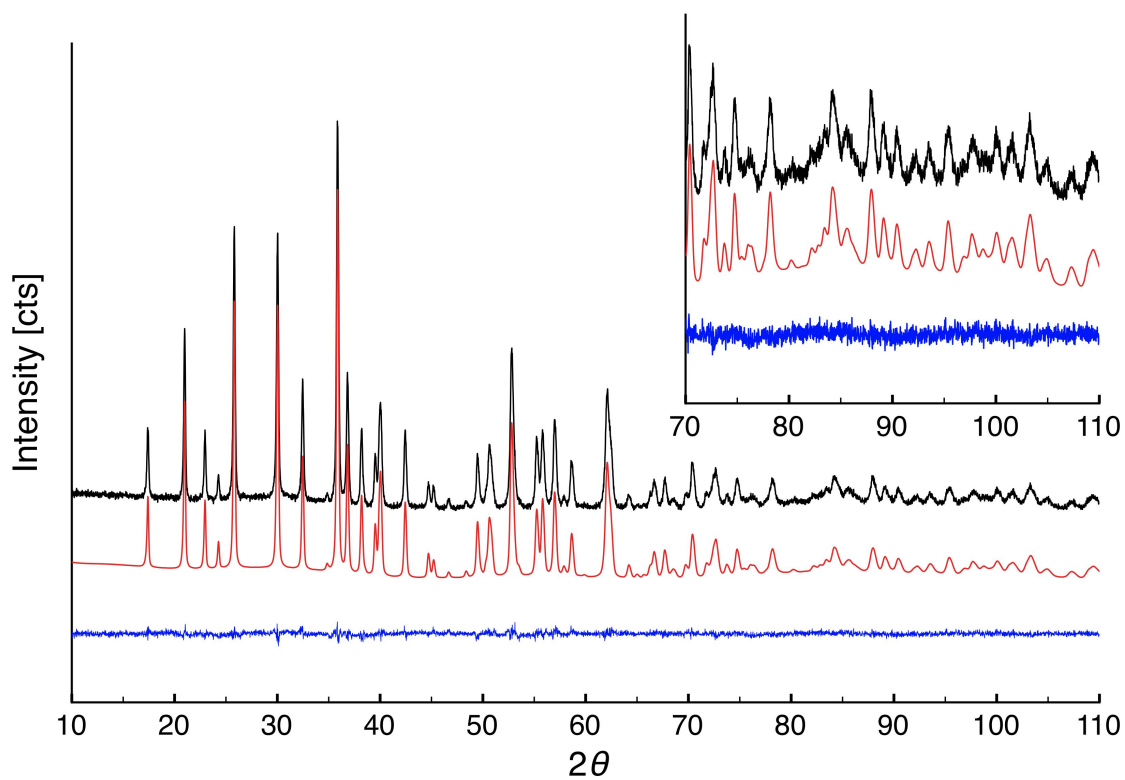


Figure S1. Observed (top, in black), calculated (middle, in red), and difference (bottom, in blue) profiles for the Rietveld refinement of undoped LiFePO_4 . The higher angle data have been scaled up to show more detail.

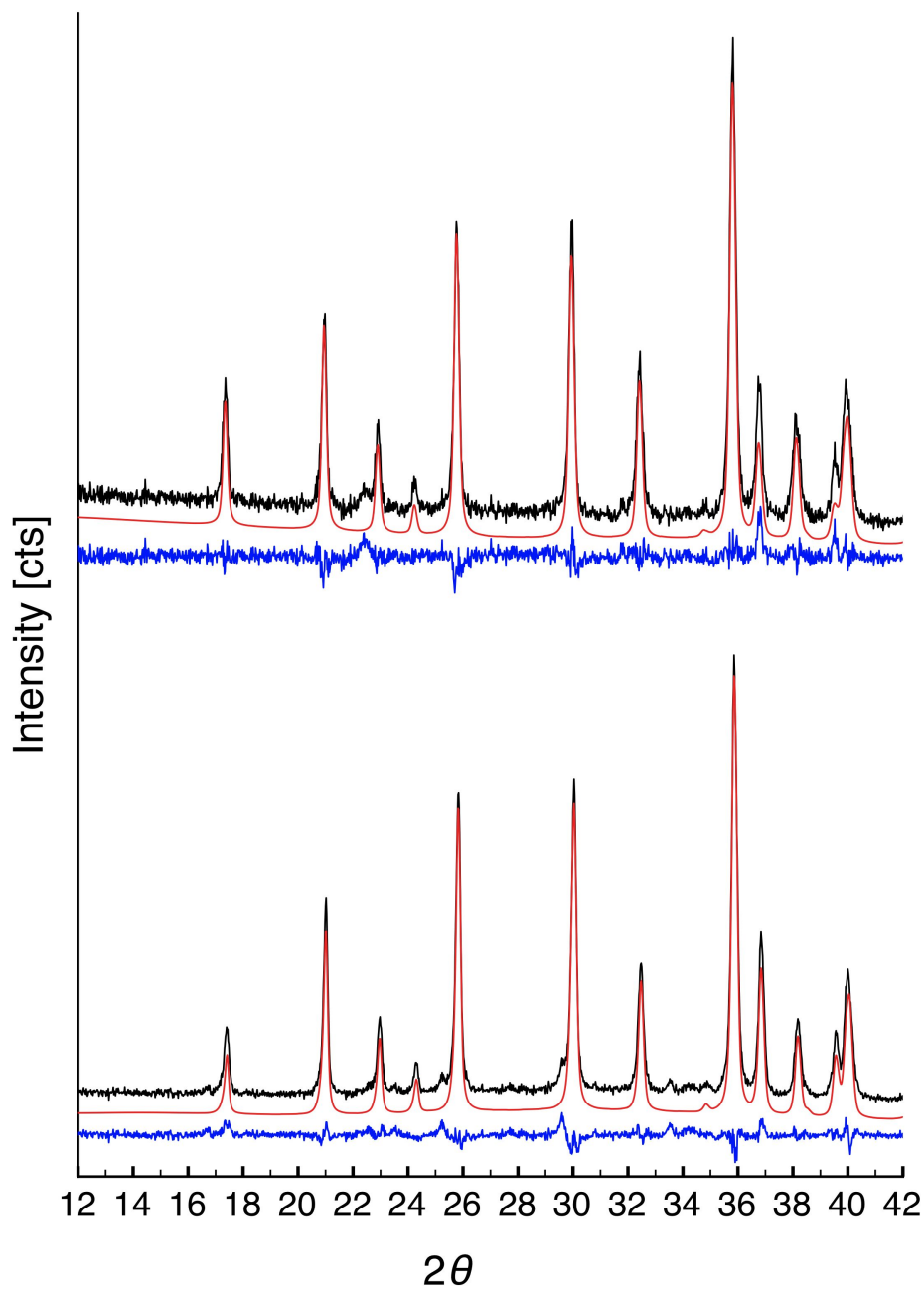


Figure S2. Observed (in black), calculated (in red), and difference (in blue) profiles for the Rietveld refinement of the doped $\text{LiZn}_{0.07}\text{Fe}_{0.93}\text{PO}_4$ (top) and $\text{LiNi}_{0.05}\text{Fe}_{0.95}\text{PO}_4$ (bottom) compounds. The impurity peaks could be clearly seen from the Rietveld refinement.

Sample	C(S1) / $\Delta\chi^2$ (S1)	C(S2) / $\Delta\chi^2$ (S2)	C(S3) / $\Delta\chi^2$ (S3)	C(S4) / $\Delta\chi^2$ (S4)
LiAl _{0.02} Fe _{0.98} PO ₄	0.037 / -0.001	0.014 / -0.001	/	0.014 / -0.001
LiMn _{0.05} Fe _{0.95} PO ₄	0.001 / 0.000	/	0.002 / 0.000	/
LiTi _{0.02} Fe _{0.98} PO ₄	0.016 / -0.001	0.012 / -0.002	0.009 / -0.002	0.013 / -0.001
LiNi _{0.07} Fe _{0.93} PO ₄	0.027 / -0.021	0.003 / +0.001	0.021 / -0.019	/
LiZn _{0.02} Fe _{0.98} PO ₄	0.003 / +0.002	0.011 / 0.000	0.006 / +0.002	/

Table S2. Refined doping concentration (C) and the variation of χ^2 assuming different doping mechanisms. $\Delta\chi^2$ is the difference between the χ^2 value obtained assuming single-phase olivine LiFePO₄ structure and the χ^2 value obtained assuming the proposed mechanism. More negative values correspond to better results. For details see main text.

Energy Dispersive X-ray Analysis

X-ray spectrum images (SIs) obtained in scanning transmission electron microscope (STEM) mode from $\text{LiZn}_{0.02}\text{Fe}_{0.98}\text{PO}_4$ and $\text{LiNi}_{0.07}\text{Fe}_{0.93}\text{PO}_4$ samples were acquired from the areas shown in Figures S1 and S2 (left). The elemental maps were extracted from the original SIs. The X-ray intensities of the characteristic $K\alpha$ lines of the elements of interest were extracted as images from the measured EDX SIs using an energy-window method, i.e. the X-ray intensities at specific characteristic peaks were obtained from the SIs by selecting the corresponding energy ranges. All analyzed lines do not overlap. Figures S1 and S2 (right) show the elemental maps of O, P, Fe and Zn/Ni $K\alpha$ lines, extracted from the EDX SIs. A homogeneous distribution of all the elements is observed on both samples. The EDX spectra of $\text{LiZn}_{0.02}\text{Fe}_{0.98}\text{PO}_4$ and $\text{LiNi}_{0.07}\text{Fe}_{0.93}\text{PO}_4$ are shown in Figure S3.

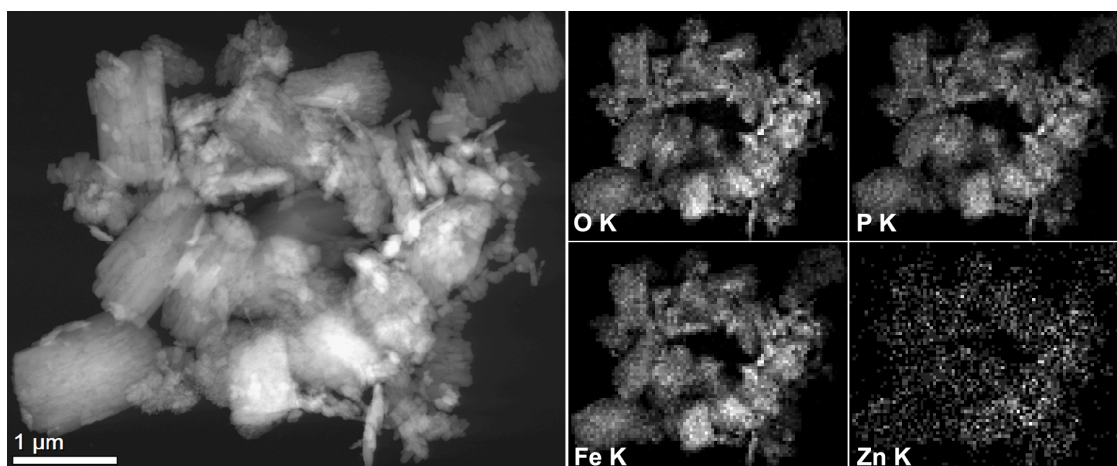


Figure S3. O, P, Fe and Zn $K\alpha$ maps of the $\text{LiZn}_{0.02}\text{Fe}_{0.98}\text{PO}_4$ sample obtained from the measured EDX SIs of the area shown at the left side.

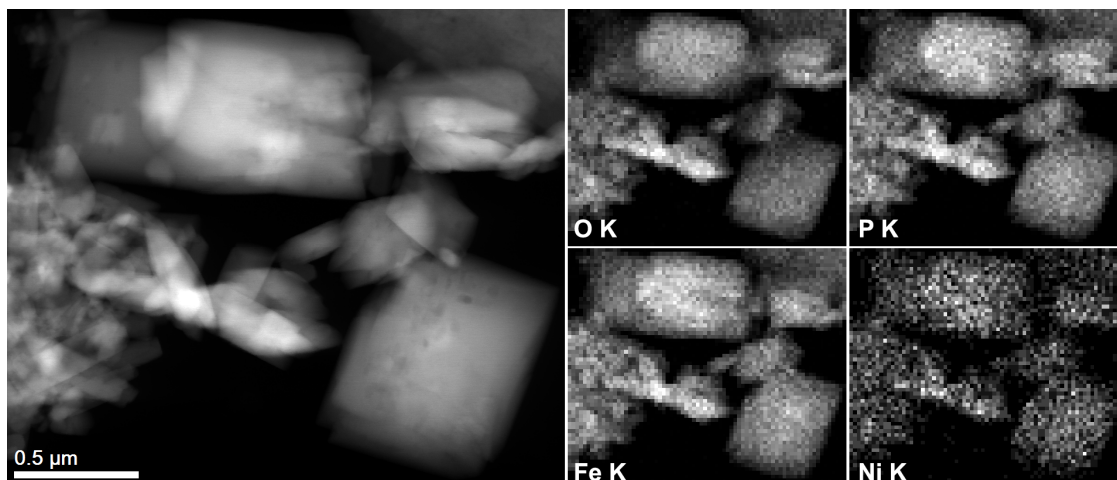


Figure S4. O, P, Fe and Ni $K\alpha$ maps of the $\text{LiNi}_{0.07}\text{Fe}_{0.93}\text{PO}_4$ sample obtained from the measured EDX SIs of the area shown at the left side.

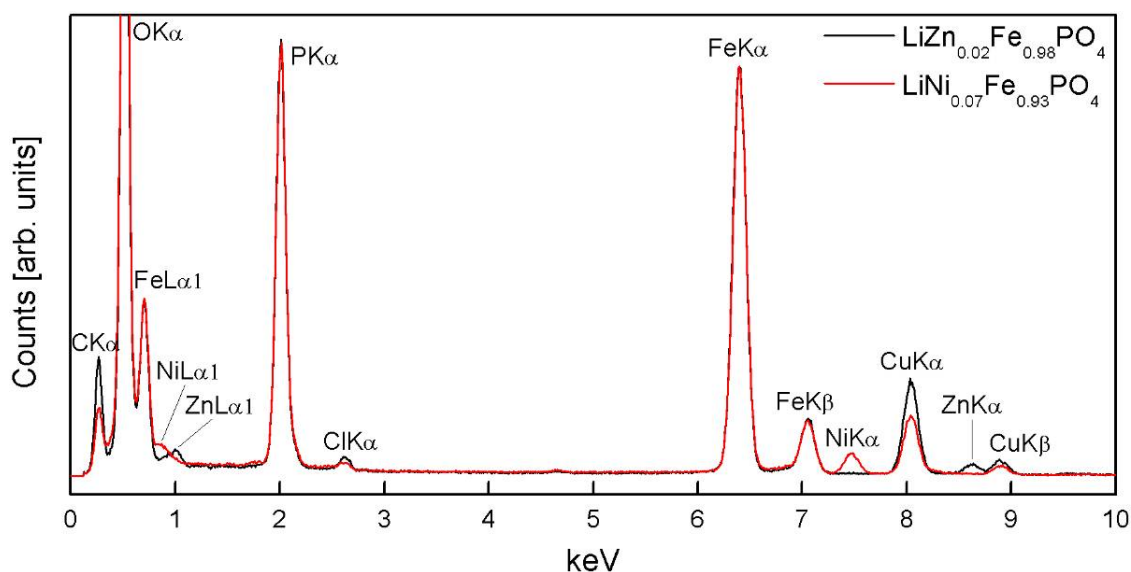


Figure S5. EDX spectra of the $\text{LiZn}_{0.02}\text{Fe}_{0.98}\text{PO}_4$ and $\text{LiNi}_{0.07}\text{Fe}_{0.93}\text{PO}_4$ samples acquired from the areas shown in Figures S1 and S2. For clarity, the EDX spectra are normalized with respect to the peak maximum of the Fe $K\alpha$ line. Small amounts of chlorine from the precursor solutions are observed. The carbon and copper signals originate from the carbon-coated copper TEM grid.